Customizable Graphite-on-Paper based Keypads: Toward Disposable and Recyclable Wireless Human-Machine Interfaces

Customizable Graphite-on-Paper based Keypads: Toward Disposable and Recyclable Wireless Human-Machine Interfaces

Muhammad Hamza Zulfiqar, Mahmood Ul Hassan, Khawaja Qasim Maqbool, Muhammad Zubair, Muhammad Qasim Mehmood, Kashif Riaz and Yehia Massoud

***Abstract*—There is a rapid increase in the use of affordable electronic devices and human-machine interfaces (HMIs) with short serviceable life in almost every aspect of our lives. It's estimated that the Waste Electrical and Electronic Equipment (WEEE) and e-waste generated in year 2021 was 57.5 million metric tons (Mt) and it is expected that the production of e-waste will increase to 110 Mt by the end of 2050. To mitigate these wastes, green HMIs are required which can be customized for multiple applications and can be recycled or disposed of with minimal environmental impact. This work presents customizable graphite-on-paper (GOP) based keypad consists of interdigitated capacitive (IDC) touch sensors is demonstrated as HMIs to interact with different electronic and media applications wirelessly. The GOP keypads are fabricated through facile and green fabrication process by direct writing of graphite on flexible paper substrate. The GOP keypads can be fabricated in a home setting as the required materials are readily available, i.e., paper, pencils, Arduino. The GOP keypads can be easily disposed of or recycled at the end of its life or requirement due to the employment of biodegradable materials like paper and graphite. The IDC touch sensors are optimized by analyzing the number of electrode fingers, finger's width, finger's overlap length and spacing between the electrode fingers. The same GOP keypad is customized to interact with different electronic and media applications wirelessly i.e., laptop cursor navigation, calculator app on mobile, numeric keypad etc. The customizable GOP keypads have potential to be used as green wireless HMIs to enforce a circular economy by mitigating electronic and plastic waste, which leads to the vision of a sustainable and green world.**

***Index Terms*— Customizable IDC electrodes, disposable keypads, flexible, green, graphite-on-paper, wireless human-machine interfaces**

I. INTRODUCTION

TECHNOLOGICAL advancements are rapidly changing the world due to an immense increase in the usage of electronic devices like IoT devices, laptops, cell phones, cameras, and HMIs [1]. According to the International Renewable Energy Agency (IRENA) report, the number of electronic devices connected to the internet worldwide would be increased to around 70 billion compared to the existing 35.8 billion devices [2]. The increase in the use of electronic devices growing the generation of electronic waste (e-waste) and causing severe environmental problems. The global e-waste generation data from the Global e-Waste Monitor from 2014 to 2030 is shown in Fig. 1 (a). The Global e-Waste Monitor is a joint venture of the Sustainable Cycles (SCYCLE) program and the International Telecommunication Union (ITU) [3]. It's estimated that the Waste Electrical and Electronic Equipment (WEEE) and e-waste generated in year 2021 was 57.5 million metric tons (Mt) [4]. The estimated weight of WEEE and e-waste was more than the Great Wall of China, the Earth's heaviest artificial object. By the end of 2050, its expected that the production of e-waste will increase to 110 Mt [5]. According to the estimates, the production of plastic waste will hit 12 billion tons by the end of 2050 [6]. About 42% of WEEE and e-waste consists of waste printed circuit boards (WPCB). According to the 2019 formal documentation, the recycling of WEEE was ~17% and major part of WEEE ~83% was not managed properly [7]. Fig. 1 (b) shows the division of 2021 WEEE into subdivisions. WEEE from small household equipment and ICT majorly consists of a waste obtained from printed circuit boards.

The WPCBs from overall WEEE, particularly from small household equipment and ICT, are rising due to the high demands [4]. The adverse impacts of WEEE on the environment are diverting the attention towards developing eco-friendly and circular sustainable electronics [8]. Along with the WEEE production, the currently available devices are rigid, indestructible, unfoldable and reluctant [4]. The evolution of electronics into non-planer and complex shapes is the need of

Corresponding authors: K. Riaz (e-mail: kashif.riaz@itu.edu.pk) Y. Massoud (e-mail: yehia.massoud@kaust.edu.sa).

M. H. Zulfiqar and M. U. Hassan contributed equally.

M. H. Zulfiqar was with MicroNano Lab, Department of Electrical Engineering, Information Technology University (ITU) of the Punjab, Ferozepur Road, Lahore 54600, Pakistan. He is now with Department of Biomedical Engineering, Narowal Campus, University of Engineering and Technology, Lahore 54890, Pakistan

M. U. Hassan, M. Zubair, M. Q. Mehmood, and K. Riaz are with MicroNano Lab, Department of Electrical Engineering, Information Technology University (ITU) of the Punjab, Ferozepur Road, Lahore 54600, Pakistan

K. Q. Maqbool is with Department of Computer Science, Bahria University, Lahore Campus, Pakistan

Y. Massoud is with The Innovative Technologies Laboratories (ITL), King Abdullah University of Science and Technology (KAUST), Thuwal 23955, Saudi Arabia (e-mail: yehia.massoud@kaust.edu.sa)

Color versions of one or more of the figures in this article are available online at http://ieeexplore.ieee.org

time to utilize the consumer electronics everywhere in human lives regardless of just straight and non-flexible substrates.

Recently, due to e-waste, WEEE and rigidity of existing electronics, a great interest has been developed in manufacturing electronics devices using flexible and green substrates using new fabrication techniques and materials. The current developments in flexible electronics open a range of new applications, including implantable electronics for biomedical, soft robotics, sustainable sensors, and energy harvesting devices, and consumer electronics [9]. Flexible electronics have shown the refreshed attention of paper as a material to be used in modern electronics because it is widely available, entirely sustainable, inexpensive, and, more importantly, has a small environmental footprint [10, 11]. Paper-based electronics or papertronics are devices with electro-chemo-optomechanical properties that allow the functionality to be printed on or within a paper-based substrate [12]. Paper is worldwide available all around us and has the potential to contribute as a substrate toward the development of green and flexible electronics. Paper as a substrate allows easy manipulations towards chemical changes, physical impact, and complex 3D formations [13-15]. Other flexible substrates like polyethylene terephthalate (PET), polydimethylsiloxane (PDMS), and polyimide (PI) are of great importance because of their flexibility, but the drawback of using these materials is the environmental pollution due to their low degradation [16-19]. Moreover, the fabrication processes required for these flexible substrates are complex, costly, and not eco-friendly. On the other hand, paper being environmentally friendly and biodegradable, is extensively used as a substrate for the development of paper-based foldable electronics such as solar cells [20], conductive traces [21], filter circuits [22], supercapacitors [23], batteries [24], transistors [25], organic electronics [26], gas sensors [27], micro droplet sensors [28], electronic memory storage [29], touch sensors [30, 31], and displays [32].

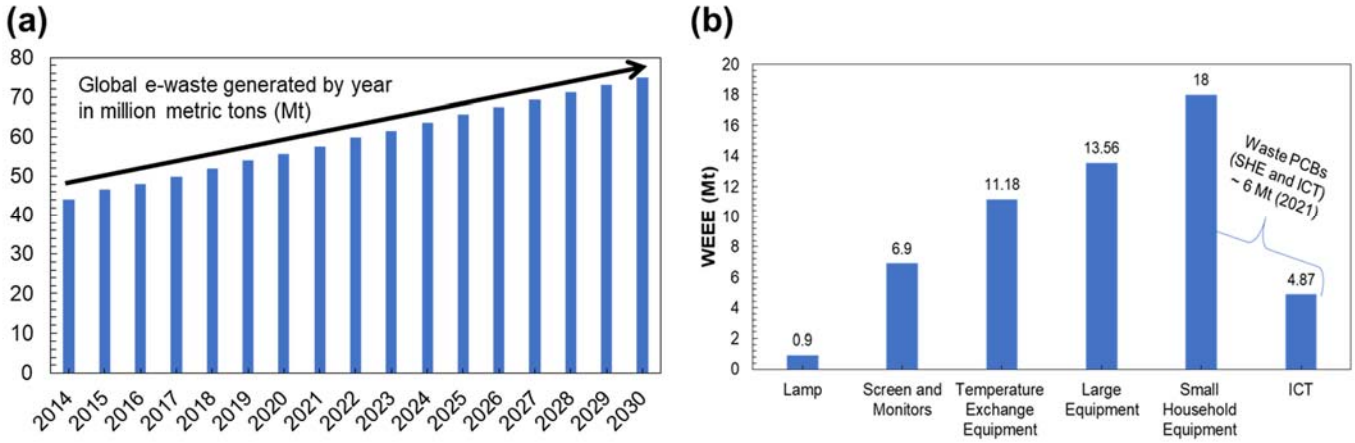

Fig. 1. Global e-waste statistics and proposed solution. (a) Global WEEE projection by years in Mt [3]. (b) Contribution of WPCBs in the year 2021 from WEEE [4].

User input is most important to enable new types of consumer products [30]. The human-machine interface (HMI) is the way to connect the user input touch keypads with electronics to get input from the end-user [33]. Integration of buttons with foldable and flexible electronics and sensors for disposable applications is not easy. Disposable HMIs can contribute to future developments in smart packaging, disposable electronics devices, intelligent labels, use-and-throw sensors systems, and touch interactive displays. However, the current market available plastic buttons and human-machine interfaces are not too thin and fabricated from expensive, hazardous materials and processes. The recent years electronic waste has been generated worldwide with on average 20% of plastic faction [34]. The recycling of e-waste and plastics in e-waste causing human health and environment issues because of heavy metals in e-waste and harmful additives in plastics of electronics [35]. This shows the need to develop environment-friendly and facile touch sensors for interface control and disposable applications as input devices. Several costly conductive materials have been used to fabricate foldable electronics and touch sensors, such as silver nanoparticle ink, silver nanowires ink Ag NWs, hydrothermally grown ZnO, and Al coated PI sheets [30, 36-39]. The preparation of these inks and materials includes multistep, solvent-based, costly procedures and diffusion of toxic liquid hazardous chemicals. All these issues limit the use of conductive ink to develop touch keypads for environmentally friendly and disposable applications. Current fabrication techniques used to fabric conventional and indestructible electronics are environmentally unfriendly and involve several gaseous and chemical procedures causing greenhouse emissions [33]. Reported foldable touch keypads fabricated using lithography, etching, screen printing, 3D printing techniques, and direct printing followed by sintering and heating to achieve higher conductivity by evaporating solvents of inks [30, 36-39]. The reported touch sensors are non-customizable and developed for just a single particular application [33]. The fabrication cost, tools, and solvents involved in the fabrication process do not result in eco-friendly and economical touch sensors and devices. A previously reported study integrated just four graphite-based sensors based non customizable keypad with Arduino using non-stable and inconsistent crocodile pins to

ON/OFF the LEDs [33]. Best of our knowledge, none of the previous reports describe an effective and consistent connection between the GOP-based sensors and electronics. Also, no previous studies describe the utilization of paper-based facile and eco-friendly touch keypads to interface them with mobiles to control mobile phones and laptops effectively.

Herein, we report a simplistic and ultra-low-cost direct writing technique to deposit conducting electrodes of GOP keypad. The GOP keypad are composed of touch sensors, and each touch sensor is a comb-type IDC electrode. The influence of different IDC sensor parameters was evaluated to develop a simplified and easily arrayed unit touch sensor. The base unit sensor was arrayed to develop four sensors-based customizable navigation key controlling navigation GOP keypad, ten sensors-based customizable numeric GOP keypad, and the fifteen touch sensors-based customizable calculator GOP keypad. The navigation GOP keypad was utilized to interface wirelessly with the laptop to control its navigation keys. Ten different LEDs was interfaced with numeric GOP keypad through wires to demonstrate the working of capacitive touch sensors-based keypad. The calculator GOP keypad was interfaced with the mobile calculator app through Bluetooth to interface and wirelessly control the Android mobile-based homemade Calculator App. The consistent electrical properties of graphite were obtained by patterning six to seven layers in designed patterns. The self-fabricated touch sensors-based keypad was integrated with Arduino to control the homemade Android-based Calculator mobile app. Fig. S1 shows the graphical illustration of the proposed system with its working principal. Delicate, slender, inexpensive, removable, and non-sticky Cling sheet deposited on graphite sensors to minimize the performance degradation of the keypad by human rub and touch as well as the environmental humidity and human sweating.

II. Materials and Methods

A. *Materials*

A standard A4 Cellulose printer paper of 80 grams with 100 µm thickness was used as a substrate for interdigitated capacitive (IDC) touch sensors based on keypads. Graphite pencils of different graphite to clay content ratios such as HB (68 ± 2%), 2B (74 ± 2%), 4B (79 ± 2%), and 8B (90 ± 2%) by MONO were used to fabricate graphite-based thin-film electrodes of IDC sensors [40]. Cling sheet was utilized for the protection of graphite from degradation to maintain the performance of GOP-based sensors. The dielectric constant of Cling sheet reduced the measured capacitance of sensor for finger touch.

B. *Sensor Fabrication*

The IDC sensor was designed in MS Word using the parameters optimized in Excel. The sensors were designed in MS Word to attain the regularity, similarity, and consistency in sensors to achieve repeatable results. The designed sensor is printed on A4 cellulose paper using an HP Desktop printer. Pictorial representation for the process of designing and printing a sensor is shown in Fig. 2 (a) and (b), respectively. Cellulose paper printed IDC sensor was fabricated using graphite-on-paper-based manual fabrication techniques. The pencil was drawn in one direction to deposit the first layer of graphite in printed patterns of a sensor, as shown in Fig. 2 (c). It's observed that the few spaces remained empty after the deposition of the first layer of graphite, and the results obtained were not repetitive and unrealistic. To achieve consistent results from graphite-based manually fabricated sensors, consistency in electrical properties of conductive layers was required. Consistency in graphite layers was achieved by penciling in different directions as layer by layer. The second layer of graphite was deposited in perpendicular to first layer, as shown in Fig. 2 (d). Seven layers of graphite were deposited in a different direction to fabricate consistent sensors for reliable and repeatable results. The sensor fabricated by depositing seven layers of graphite is shown in Fig. 2 (e). GOP based fabrication process is solvent free and does not include any adhesive, solvent, and stickiness materials to deposit graphite throughout the fabrication of sensors. The graphite act as conductive materials and areas of sensors includes the graphite called electrodes. The performance of graphite decreased with a human touch by rubbing the graphite from the conductive traces. To address the performance degradation issue of graphite, a transparent and removable Cling sheet was utilized as protection on fabricated sensors as shown in Fig. 2 (f). A thin HYGEN Cling sheet was used as a protection sheet to prevent the performance degradation of graphite sensors from human touch.

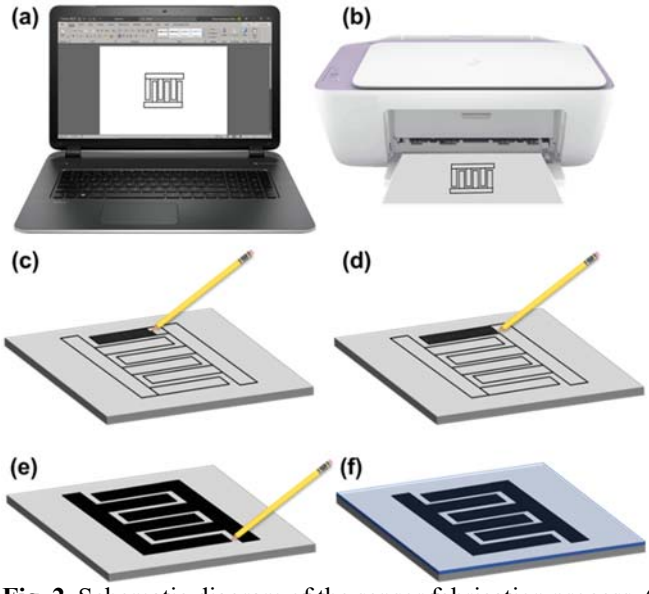

Fig. 2. Schematic diagram of the sensor fabrication process. (a) Designing of sensors using MS word for optimized and selected sensors dimensions. (b) Printing of sensor design on paper using HP inkjet printer. (c) Direct writing based deposition of the first layer of GOP. (d) Direct writing of the second layer of GOP perpendicular to the first layer. (e) Sensor fabricated after deposition of seven layers of GOP in different directions. (f) Graphite-based fabricated sensor with thin Cling sheet as a protection sheet.

C. Characterization

The change in capacitance of interdigitated sensor was utilized to differentiate between the touch and no-touch conditions. The capacitance change was measured and identified through the sensor's integration with Arduino Mega 2560 development board. The sensors were integrated with Arduino at analog ports, and capacitance was measured through the RC characteristics. The Internal resistance of Arduino was used to measure capacitance for all the sensors. In addition, the Arduino was integrated with Android mobile through an HC Bluetooth module to control the facile sensor's machine interface wirelessly. The Arduino was also connected with the LCD to show the sensors working through wires. The complete characterization and experimental setup include the Arduino Mega integrated with input sensors, LCD, and mobile is shown in Fig. S2.

III. RESULTS AND DISCUSSION

Touchpads with resistive [41], capacitive [30, 33, 36, 38], infrared [42], and triboelectric [43, 44] sensing protocols developed. These developed touchpads were used to collect the keystrokes from the users. Most of the newly developed consumer products will require different user interfaces depending upon the applications. Resistive touchpads are developed to detect resistance changes with human interaction with simple circuits. The results of these touchpads are less repeatable and less sensitive [45]. However, resistive touch screens are used in the mobile phones of Nokia and Samsung. Infrared touch sensors detect the touch by the change in intensity of infrared light because of human interaction with the highest sensitivity, but the issues liked with this scheme are complex, environmentally unfriendly, and costly fabrication process, and high-power utilization [36]. The triboelectric touchpads consist of active sensors, but the scheme requires high cost and special materials for fabrication. Comparatively, the capacitive touch sensing scheme has become more popular due to higher repeatability and sensitivity, low power utilization, and fab-lab-free fabrication.

Current touch keypads are based on costly and special conductive material with smooth surface-based polymer substrates that are not best suitable for foldable applications. Special fabrication techniques are required to deposit these materials on substrates for touch keypad manufacturing. In this context, paper, pencil, and garage fabrication are best suitable for manufacturing facile, eco-friendly, flexible, thin, and lightweight touchpads for highly repeatable and highly sensitive results towards the human touch.

Capacitive touch keypads can be of two types based on electrode structure for capacitive sensors as parallel plate or in-plane. The parallel plates based capacitive sensors exhibit less repeatable and sensitive results for human touch. In-plane capacitive sensors are also called interdigitated capacitive (IDC) sensors based on the design of plates of the sensors. In structure, both electrodes of the capacitive sensor are in a plane in a comb-based scheme that contains one or more capacitor electrodes in the touch area to register the human touch by detecting the change in capacitance. The in-plane capacitors demonstrate the smaller base values of capacitive sensors for no-touch conditions, but it's more sensitive than parallel plate because of 1-2 orders increase in the capacitance for touch conditions. IDC sensors scheme allows the 2D fabrication on any single side of the paper and, therefore, the in-plane scheme-based IDC sensors utilized in this work.

The schematic view of IDC sensors representing its components is shown in Fig. 3 (a). The capacitance calculation of IDC comprises the capacitance of unit cells and is calculated using the expression 1 [46, 47].

$$C = C_{UC}\,(N-1)\,L \tag{1}$$

where C is the total capacitance, C_{UC} is the capacitance of any unit cell, N is the count of unit cells/electrodes, and L is the overlapped length of capacitor electrodes [47]. The capacitance of a one-unit cell further consists of three different capacitances as C_1 over the surface of the electrodes, C_2 in between the electrodes, and C_3 under the electrode surface. The capacitance of the unit cell is expressed in expression 2 [47]. Expression 3 represents the capacitance of C_1 and C_3, and expression 4 represents the capacitance C_2. C_1 and C_3 are the same other than dielectric materials because of the same elliptical patterns of electric field lines of capacitor electrodes, as shown in Fig. 3 (b).

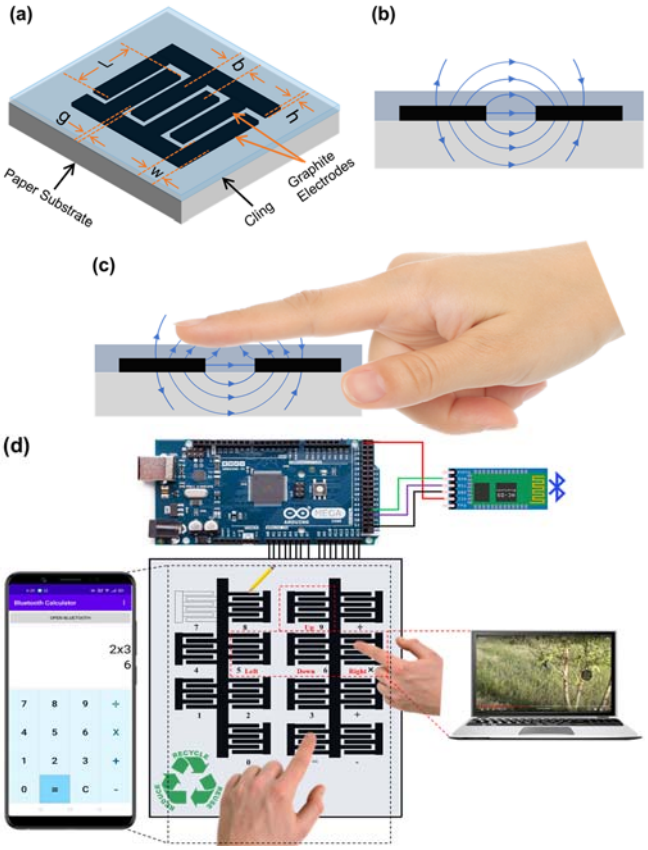

Fig. 3. Paper-based capacitive touch sensor. (a) A graphic view of paper-based IDC touch sensor. (b). Cross-sectional schematic of capacitive touch sensor represents the working in no-touch and (c) touch condition. (d) Pictorial representation of

working of reported disposable and green customizable sensors working with mobile and laptop through Bluetooth.

$$C_{UC} = C_1 + C_2 + C_3 \quad (2)$$

$$C_1 + C_3 = \varepsilon_o \left(\frac{\varepsilon_1 + \varepsilon_3}{2}\right) \frac{K\sqrt{1-(g/w)^2}}{K(g/w)} \quad (3)$$

$$C_2 = \varepsilon_o \varepsilon_2 \frac{h}{g} \quad (4)$$

where ε_o is the dielectric constant of free space, ε_1 is the dielectric constant above the electrode surface, ε_2 is the dielectric constant in-between electrodes, ε_3 is the dielectric constant underneath the electrodes, K (g/w) is the complete elliptical integral of the first kind, g is the spacing between the electrodes, w is the width of one-unit cell, h is the thickness /height of electrode. Fig. 3 (b) shows the electric field lines of the sensor electrode pass the cling protection and substrate elliptically. The IDC works as sensors when any other materials contact the field lines. The dielectric constant of the in-contact materials changes the capacitance and sense exits. A cross-sectional view for the interaction of the human finger with electric field lines of IDC sensors is shown in Fig. 3 (c). Working of GOP-based disposable and green customizable sensors-based calculator and navigation HMIs for Calculator App and laptop is shown in Fig. 3 (d). Reported GOP-keypads are customizable because of reconfiguration in software to use the sensors for the targeted application as required instead of hardwired as well as the sensors can be fabricated for different geometries as well as different numbers quantitively are per the requirements.

The functionality of the touch sensors was measured using the Arduino Uno and Mega development boards. The effect of length, width, and the number of electrodes and spacing between the electrodes evaluated to finalize the dimensions of sensors to get higher sensitivity with appropriate size compared to the finger size. Three sensors for each data point of subparts of Fig. 4 were fabricated and evaluated. The fabricated sensors for all the data points were tested for the capacitance measurement was measured in un touch state (MIUS) and measured in touch state (MITS). The calculations for the different parameters of IDC were performed in MS Excel. Fig. 4 (a) shows the calculated and measured capacitance in un touch (MIUS) and touch (MITS) states of the IDC sensor for different electrode lengths. The length of the electrode directly relates to overall capacitance, and the increase in length increases the capacitance. The effect of the number of pairs of fringes on IDC evaluated through calculation, MIUS, and MITS is shown in Fig. 4 (b). Fig. 4 (c) and (d) show the effect of the increase in spacing between the electrodes and the increase in the width of electrodes. Measured results are greater than calculated results because of parasitic capacitances added to sensors actual capacitance while capacitance measurements through Arduino.

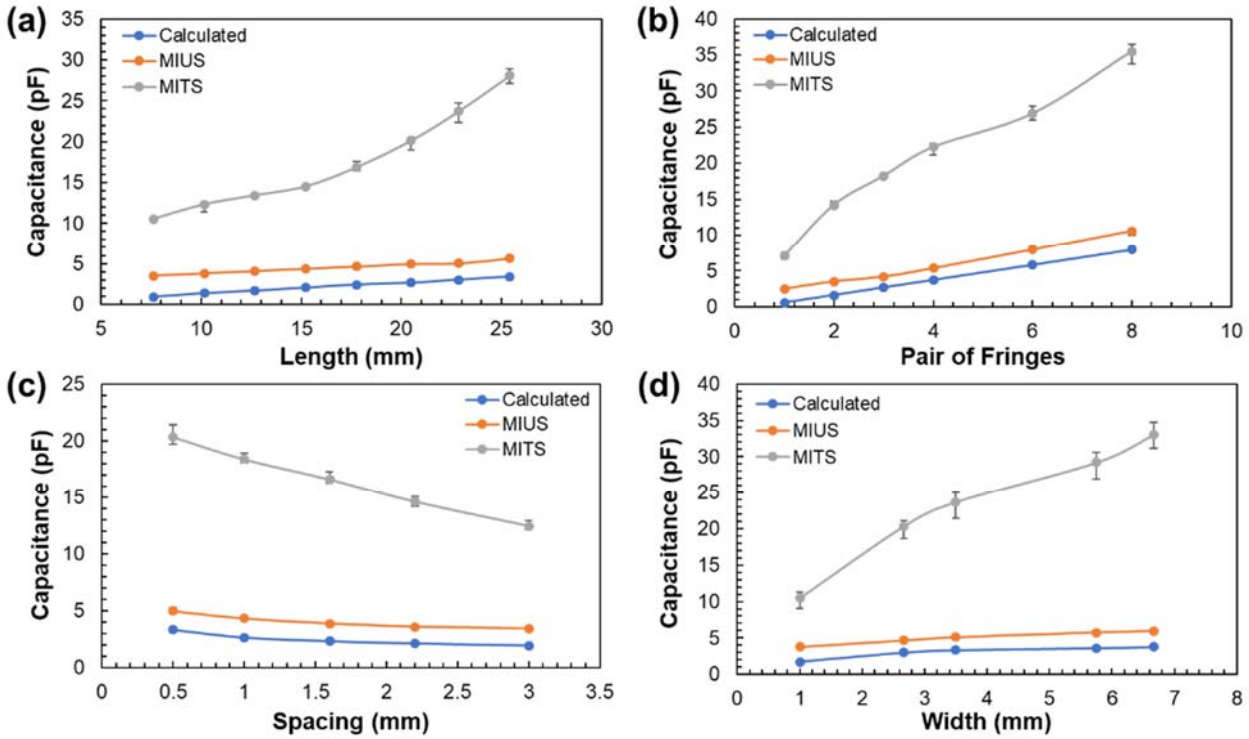

Fig. 4. IDC parameters influence capacitance in calculation and measured results in un touch and touch conditions. (a) Influence of increase in common length of electrodes. (b) Influence of increase in the number of electrodes. (c) Effect of increase in spacing between the electrodes. (d) Effect of increase in width of electrodes.

The IDC sensor was evaluated for different graphite to content ratio pencils. Three sensors for each graphite pencils as 2B, 4B, 6B, and 8B, were fabricated, and the measured capacitance of IDC for touch and no-touch conditions is shown in Fig. S3. Looking into the capacitance measured for different parameters of IDC and the average size of human fingers, we finalized the sensor design with 6 electrode fingers with 17 mm common length (L), 2.5 mm width (w), and 1 mm space (G)

between the fingers. 8B pencil utilized throughout to fabricate sensors to achieve highly decisive results. The photo of IDC fabricated from 8B pencil with L = 17 mm, W = 2.5 mm, and G = 1 mm is shown in Fig. 5 (a). The capacitance of IDC was measured through NI Elvis and Arduino development boards. The results of a single bare sensor tested in touch and no-touch states multiple times is shown in Fig. 5 (b). Usually, the real human finger exhibits surface moisture, and it degrades the performance of graphite-based electrodes due to the direct interaction in the longer run. The use of a protection sheet on graphite electrodes also decreases the effect of the finger on the change of capacitance of a capacitor with a touch state. Looking into the performance degradation and effectiveness in response of sensors towards the touch, we safely introduced a Cling sheet-based ultra-thin protection sheet in our work. The presence of the Cling sheet on the sensor is represented through the model shown in Fig. 3 (a). Fig. 5 (c) shows the photo of the fabricated IDC with a Cling sheet. The capacitance of Cling protected IDC for touch and no-touch states are shown in Fig. 5 (d). Touch and no touch states of bare and shielded sensors evaluated through rigorous testing for the decision of threshold value of capacitance for touch and no-touch. The black line in Fig. S5 (b) and (d) shows the threshold at 8 pF for both the bare and shielded sensors.

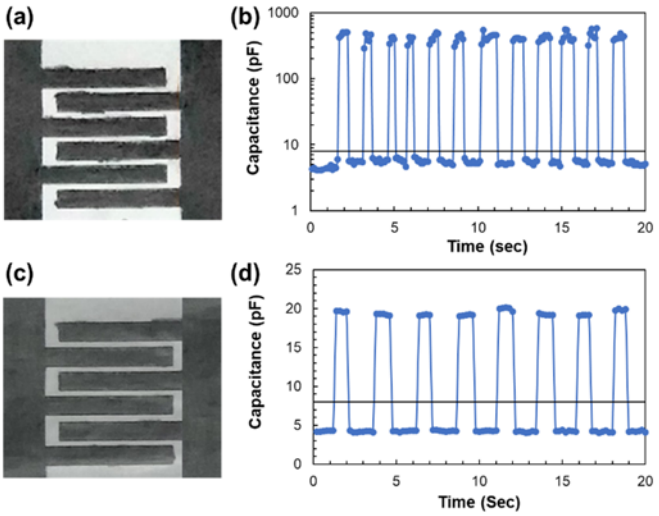

Fig. 5. IDC sensor fabricated with GOP-based fabrication process. (a) Photo of the fabricated bare sensor. (b) The measured capacitance of bare sensor in touch and no-touch state. (c) Photo of Cling sheet shielded sensor. (d) The measured capacitance of the shielded sensor in touch and no-touch state.

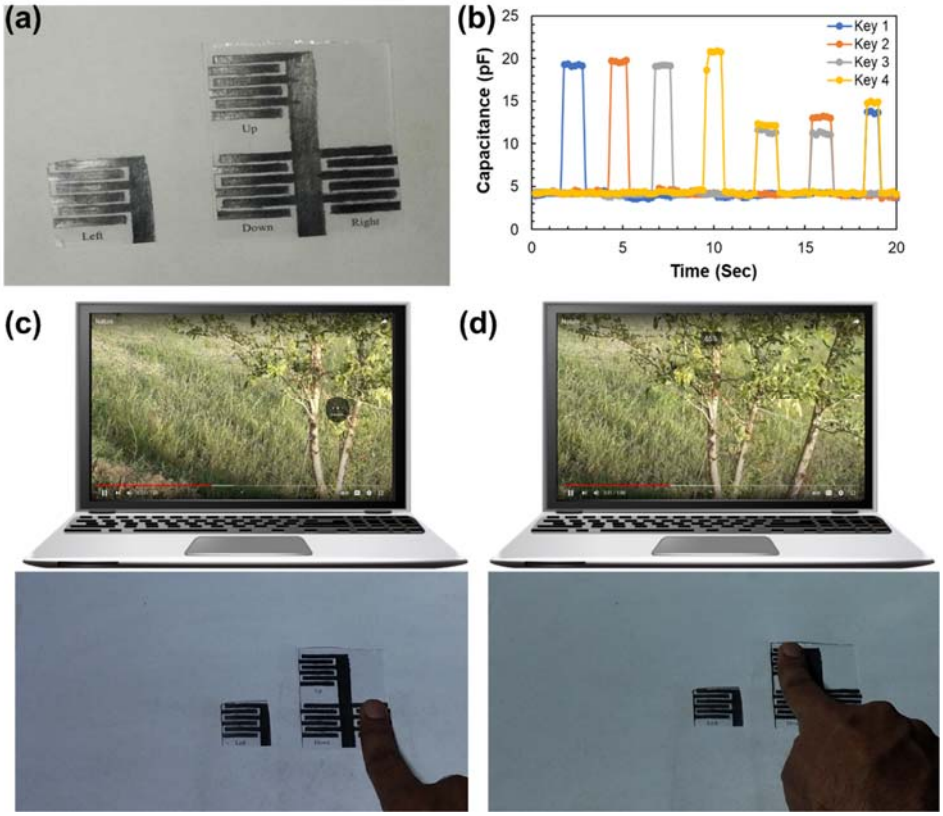

Fig. 6. Laptop's Navigation keys controlling navigation GOP keypad. (a) Photo of graphite on the paper-based fabricated navigation GOP keypad. (b) The capacitance of the keys of the keypad in touch and no-touch states. (c) Photo of finger touch on right key and (d) up key of the keypad for 5 seconds forwarding and 5 % volume up of YouTube video.

The performance of touch sensors was studied through the development of four sensors-based touchpads. The touchpad was designed in MS word, printed on paper through a printer, and fabricated through the 8B pencil using graphite on the paper-based fabrication process. The sensors electrodes connected with Arduino through the direct exposure of thin copper wires with electrodes and then their soldering with laminated jumper wires. The practicability of the touchpad was

evaluated through functional connectivity with a laptop as a keyboard's navigation key. The touchpad sensors were named with left, right, up, and down to correspond with the navigation keys of the keypad. The photo of GOP-based navigation keys controlling navigation GOP keypad is shown in Fig. 6 (a). The sensors were connected to the Espressif Systems (ESP), and ESP was connected with the laptop through Bluetooth. Fig. S4 shows the photo of a navigation GOP keypad in connection with a laptop through Bluetooth. The behavior of sensors of navigation GOP keypads was individually evaluated for touch and no-touch states. The capacitance pattern of the keypad for touch and no touch is shown in Fig. 6 (b). When the touch of a finger with any of the keypad sensors exists, the capacitance crosses the threshold, and touch exists. Touch for any key exists continuously when the finger is in touch with respective sensors, and the key shifts to the no-touch state as the finger goes in no-touch condition from the respective sensor. The keys of the keypad were also evaluated for the simultaneous touch of two different sensors at a time; the sensor's capacitance crossed the threshold for both and performed the touch accurately. Validity of the keypad evaluated through the real-time control of navigation keys of the laptop. YouTube video controlled for forward, backward, volume up and down through the right, left, up and down keys of navigation GOP keypad respectively. Fig. 6 (c) shows the finger touch on the right key of the keypad, and the video was forwarded for 5 seconds in response. The volume up of the YouTube video was controlled through the touch of the up key of the keypad, as shown in Fig. 6 (d). Fig. S5 (a) and (b) show the 5% volume decrease and 5 seconds backward functionality of Youtube video because of the finger touch with down and left navigation keys of the navigation GOP keypad, respectively. The complete functionality of the navigation GOP keypad for volume up and down, video forward and backward of a Youtube video is demonstrated in Video S1.

To demonstrate the viability of touch sensors for more than four sensors, we fabricated ten keys-based numeric GOP keypad for 0 – 9 numbers. Designed sensors printed on paper through the printer and fabricated through GOP-based technique using 8B pencil—the sensors were connected to the Arduino through the jumper wires. The photo of fabricated numeric GOP keypad in connection with LEDs respective to individual sensors and LCD is shown in Fig. S6. The capacitance response of ten keys of numeric GOP keypad with time for touch and no-touch states is shown in Fig. 7 (a). Whenever the finger touch interaction exists with the sensor, the sensor's capacitance increases from the threshold, and touch gets registered. The keypad was also evaluated through simulations detection of two different sensors touch, and the keypad responded effectively. The workability of touch sensors evaluated through the connection of ten different LEDs with Arduino respective to each touch. LCD was also connected with Arduino to register the number of the sensor for which the touch exists. Fig. 7 (b) shows the finger touch with the numeric GOP keypad's sensor corresponding to "4", the number "4" register on LCD, and the blue LED corresponding to the sensor get on. The photo of simultaneous touch of two fingers on two sensors keys as "6" and "3" and response of touch keys on LCD and respective LEDs as shown in Fig. S7. Working of numeric GOP keypad for all the sensors keys "0,1,2,3,4,5,6,7,8,9" is demonstrated in the Video S2.

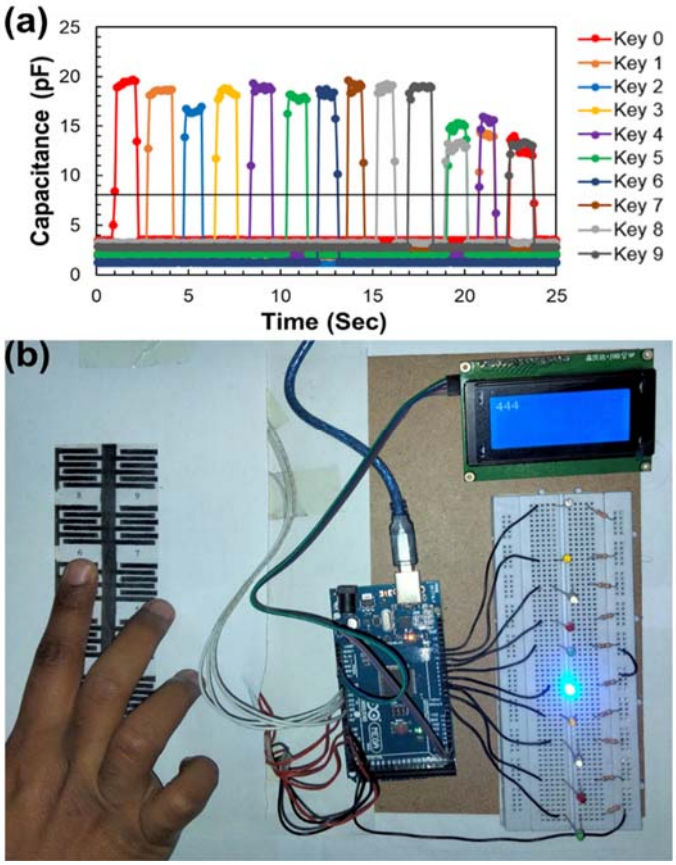

Fig. 7. Numeric GOP keypad. (a) Measured capacitance response of 10 keys of the keypad for touch and no-touch states. (b) Photo of GOP-based fabricated numeric GOP keypad being touched with a bare finger on key 4 and its response on LCD and corresponding LED.

The GOP-based keypads described in this work may be useful for developing disposable human-machine interfaces. To demonstrate an implementation of HMI, we designed a calculator GOP keypad that includes the sensors keys corresponding to the numeric and basic arithmetic operations. The keypad was fabricated through GOP-based fabrication and connected through jumper wires to the Arduino. We developed a Bluetooth-based homemade Android mobile app named "Bluetooth Calculator" to present the functionality of the calculator GOP keypad for HMI. The screenshot of homemade Bluetooth Calculator mobile app is shown in Fig. S8. The calculator GOP keypad was connected with the mobile and app through the I2C Bluetooth module connected with Arduino. Photo of calculator GOP keypad connected with Bluetooth Calculator mobile app is shown in Fig. S9. Initially, the Bluetooth of mobile has to be connected with the I2C module. Open Bluetooth button on Bluetooth Calculator app was created for the easy connection of Bluetooth of mobile with the module. When the Bluetooth initially gets connected, the touch response of the keypad gets registered on the mobile app through writing on display and bling the corresponding number or arithmetic

operation on the Bluetooth Calculator app. The sensor key corresponding to equal "=" demonstrates the functionality of answering the two register numbers concerning the registered arithmetic operation. Photo of touch on equal "=" sensor key to get the answer of two different numbers with the addition "+", subtraction "-", and multiplication "×" arithmetic operation is shown in Fig. S8 (a), (b), and (c) respectively. Bluetooth Calculator app response for touch on one numeric sensor key "5" and division arithmetic key "÷" is shown in Fig. S8 (d) and (e), respectively. Photo of finger touch on equal "=" sensor key to compute the result of two operands as 56 and 2 by division "÷" operand to get the result is shown in Fig. 8 (f). Complete operation for the division of two operands is demonstrated in Video S3. Fig. S10 shows the photos of touch inputs for the complete process of subtraction between two operands. The clear key "C" on the Bluetooth Calculator app was created to clear the computed results for the next operation or just when required. Video S4 includes the complete working of calculator GOP keypad and mobile app for the addition of two operands, "12 and 45" and the use of the clear key of the Bluetooth Calculator mobile app.

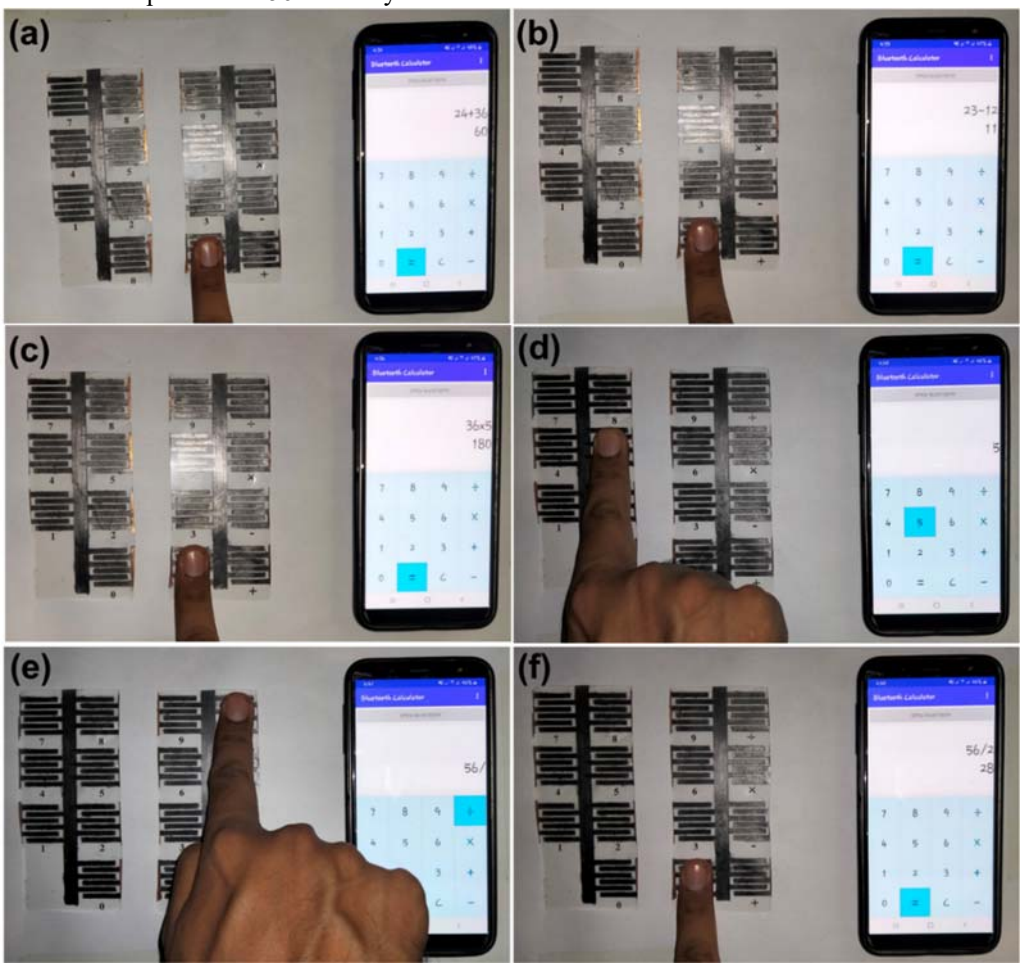

Fig. 8. Calculator GOP keypad and Bluetooth Calculator mobile app. (a) Photo of GOP-based fabricated calculator GOP keypad with the mobile app for computation of two numbers through addition operand. (b) Photo of result for the subtraction of two operands. (c) Photo of result computation for the multiplication operation. (d) Photo of numeric "5" input for the mobile app through the fabricated keypad. (e) Photo of division "÷" operand input on the mobile app through the touch of respective sensor key of the fabricated keypad. (f) Photo of finger touch on "=" sensor key to compute the result for the division operation of "56" and "2" operands.

IV. Conclusion

GOP keypads provided a facile solution to interface the electronics. The proposed IDC-based GOP keypads in this work are too thin as a simple paper, lightweight, reliable, disposable, and can consist of arrays based on the requirement. The performance of GOP keypads proved that these are a reliable alternative for the actual plastic electronics interfaces and buttons. The direct writing-based fabrication process of the keypads is inexpensive due to the utilization of economical and readily available materials such as graphite pencil and cellulose paper. The fabricated keypads work on the variations in capacitance with touch, where paper works as a substrate. The proposed keypads are customizable to be utilized for different applications. The fabricated paper-based HMIs successfully demonstrated the numeric GOP keypad to control the respective LEDs, navigation GOP keypad-based keys control of the laptop keyboard, and calculator GOP keypad for the Bluetooth calculator mobile app. The keypads demonstrate their

practicability effectively for different wireless HMI applications. Therefore, the paper has too much potential to contribute to future developments in flexible and wearable electronics and sensors. The GOP-based sensor keypads demonstration shows that these can be used in diverse applications.

ACKNOWLEDGMENT

We would like to thank Muhammad Usman Qadir and Muhammad Jaleel for their kind support.

REFERENCES

[1] D. Dias and J. J. S. Paulo Silva Cunha, "Wearable health devices—vital sign monitoring, systems and technologies," vol. 18, no. 8, p. 2414, 2018.
[2] S. Ratka, A. Anisie, F. Boshell, and N. Goussous, "Innovation Landscape Brief: Internet of Things," ed: IRENA, 2019.
[3] V. Forti, C. P. Balde, R. Kuehr, and G. Bel, "The Global E-waste Monitor 2020: Quantities, flows and the circular economy potential," 2020.
[4] M. Chakraborty, J. Kettle, and R. J. I. J. o. F. E. Dahiya, "Electronic Waste Reduction through Devices and Printed Circuit Boards designed for Circularity," 2022.
[5] W. Li and V. J. S. o. t. T. E. Achal, "Environmental and health impacts due to e-waste disposal in China–A review," vol. 737, p. 139745, 2020.
[6] R. Geyer, J. R. Jambeck, and K. L. J. S. a. Law, "Production, use, and fate of all plastics ever made," vol. 3, no. 7, p. e1700782, 2017.
[7] C. Y. Yuan, H. C. Zhang, G. McKenna, C. Korzeniewski, and J. J. T. I. J. o. A. M. T. Li, "Experimental studies on cryogenic recycling of printed circuit board," vol. 34, no. 7, pp. 657-666, 2007.
[8] A. K. Awasthi, J. Li, L. Koh, and O. A. J. N. E. Ogunseitan, "Circular economy and electronic waste," vol. 2, no. 3, pp. 86-89, 2019.
[9] D. Baran, D. Corzo, and G. T. J. F. i. E. Blazquez, "Flexible electronics: Status, challenges and opportunities," vol. 1, p. 2, 2020.
[10] R. Martins, I. Ferreira, and E. J. p. s. s. R. R. L. Fortunato, "Electronics with and on paper," vol. 5, no. 9, pp. 332-335, 2011.
[11] D. Tobjörk and R. J. A. m. Österbacka, "Paper electronics," vol. 23, no. 17, pp. 1935-1961, 2011.
[12] S. Veeralingam, P. Sahatiya, and S. J. I. S. J. Badhulika, "Papertronics: Hand-Written MoS_2 on Paper Based Highly Sensitive and Recoverable Pressure and Strain Sensors," vol. 21, no. 7, pp. 8943-8949, 2021.
[13] A. C. Glavan et al., "Omniphobic "RF paper" produced by silanization of paper with fluoroalkyltrichlorosilanes," vol. 24, no. 1, pp. 60-70, 2014.
[14] Y. Zhang, C. Lei, and W. J. A. P. L. Soo Kim, "Design optimized membrane-based flexible paper accelerometer with silver nano ink," vol. 103, no. 7, p. 155_1, 2013.
[15] X. Liu, M. Mwangi, X. Li, M. O'Brien, and G. M. J. L. o. a. C. Whitesides, "based piezoresistive MEMS sensors," vol. 11, no. 13, pp. 2189-2196, 2011.
[16] I. Taniguchi, S. Yoshida, K. Hiraga, K. Miyamoto, Y. Kimura, and K. J. A. C. Oda, "Biodegradation of PET: current status and application aspects," vol. 9, no. 5, pp. 4089-4105, 2019.
[17] U. Hassan, M. H. Zulfiqar, M. M. U. Rahman, and K. Riaz, "Low cost and flexible sensor system for non-invasive glucose in-situ measurement," in 2020 17th International Bhurban Conference on Applied Sciences and Technology (IBCAST), 2020, pp. 187-190: IEEE.
[18] M. Amjadi, K. U. Kyung, I. Park, and M. J. A. F. M. Sitti, "Stretchable, skin-mountable, and wearable strain sensors and their potential applications: a review," vol. 26, no. 11, pp. 1678-1698, 2016.
[19] W. A. D. M. Jayathilaka et al., "Significance of nanomaterials in wearables: a review on wearable actuators and sensors," vol. 31, no. 7, p. 1805921, 2019.
[20] M. C. Barr et al., "Direct monolithic integration of organic photovoltaic circuits on unmodified paper," vol. 23, no. 31, pp. 3500-3505, 2011.
[21] W. J. Hyun, O. O. Park, and B. D. J. A. M. Chin, "Foldable graphene electronic circuits based on paper substrates," vol. 25, no. 34, pp. 4729-4734, 2013.
[22] M. H. Zulfiqar, A. Alam, M. M. Saleem, M. Zubair, M. Q. Mehmood, and K. J. C. Riaz, "Tunable and foldable paper-based passive electronic components and filter circuits," vol. 28, no. 15, pp. 9959-9970, 2021.
[23] M. H. Zulfiqar, K. Riaz, and T. Tauqeer, "Foldable, Eco-Friendly and Easy Go Designed Paper Based Supercapacitor: Energy storage Device," in 2020 17th International Bhurban Conference on Applied Sciences and Technology (IBCAST), 2020, pp. 40-43: IEEE.
[24] Q. Cheng et al., "Folding paper-based lithium-ion batteries for higher areal energy densities," vol. 13, no. 10, pp. 4969-4974, 2013.
[25] W. Dou, L. Qiang Zhu, J. Jiang, and Q. J. A. P. L. Wan, "Flexible protonic/electronic coupled neuron transistors self-assembled on paper substrates for logic applications," vol. 102, no. 9, p. 093509, 2013.
[26] F. Eder, H. Klauk, M. Halik, U. Zschieschang, G. Schmid, and C. J. A. P. L. Dehm, "Organic electronics on paper," vol. 84, no. 14, pp. 2673-2675, 2004.
[27] J. Zhang et al., "Pencil-trace on printed silver interdigitated electrodes for paper-based NO2 gas sensors," vol. 106, no. 14, p. 143101, 2015.
[28] M. H. Zulfiqar, M. M. Saleem, M. Zubair, M. Q. Mehmood, and K. Riaz, "Foldable, Eco-Friendly and Low-Cost Microfluidic Paper-Based Capacitive Droplet Sensor," in 2020 International Conference on UK-China Emerging Technologies (UCET), 2020, pp. 1-4: IEEE.
[29] H. C. Chang, C. L. Liu, and W. C. J. A. f. m. Chen, "Flexible nonvolatile transistor memory devices based on One-Dimensional electrospun P3HT: Au hybrid nanofibers," vol. 23, no. 39, pp. 4960-4968, 2013.
[30] A. D. Mazzeo et al., "Paper-based, capacitive touch pads," vol. 24, no. 21, pp. 2850-2856, 2012.
[31] M. H. Zulfiqar, M. U. Hassan, M. Zubair, M. Q. Mehmood, and K. J. I. S. L. Riaz, "Pencil-on-Paper-Based Touchpad for Ecofriendly and Reusable Human–Machine Interface," vol. 5, no. 5, pp. 1-4, 2021.
[32] J.-Y. Kim et al., "Paper as a substrate for inorganic powder electroluminescence devices," vol. 57, no. 6, pp. 1470-1474, 2010.
[33] S. Kanaparthi, S. J. S. Badhulika, and A. B. Chemical, "Low cost, flexible and biodegradable touch sensor fabricated by solvent-free processing of graphite on cellulose paper," vol. 242, pp. 857-864, 2017.
[34] M. A. Butturi, S. Marinelli, R. Gamberini, and B. J. T. Rimini, "Ecotoxicity of plastics from informal waste electric and electronic treatment and recycling," vol. 8, no. 4, p. 99, 2020.
[35] M. Schlummer, L. Gruber, A. Mäurer, G. Wolz, and R. J. C. Van Eldik, "Characterisation of polymer fractions from waste electrical and electronic equipment (WEEE) and implications for waste management," vol. 67, no. 9, pp. 1866-1876, 2007.
[36] R.-Z. Li, A. Hu, T. Zhang, K. D. J. A. a. m. Oakes, and interfaces, "Direct writing on paper of foldable capacitive touch pads with silver nanowire inks," vol. 6, no. 23, pp. 21721-21729, 2014.
[37] X. Li, Y.-H. Wang, C. Zhao, X. J. A. a. m. Liu, and interfaces, "Based piezoelectric touch pads with hydrothermally grown zinc oxide nanowires," vol. 6, no. 24, pp. 22004-22012, 2014.
[38] N. M. Nair, K. Daniel, S. C. Vadali, D. Ray, P. J. F. Swaminathan, and P. Electronics, "Direct writing of silver nanowire-based ink for flexible transparent capacitive touch pad," vol. 4, no. 4, p. 045001, 2019.
[39] S. Palanisamy, M. Thangaraj, K. Moiduddin, and A. M. J. C. Al-Ahmari, "Fabrication and Performance Analysis of 3D Inkjet Flexible Printed Touch Sensor Based on AgNP Electrode for Infotainment Display," vol. 12, no. 3, p. 416, 2022.
[40] M. C. Sousa and J. W. Buchanan, "Observational models of graphite pencil materials," in Computer Graphics Forum, 2000, vol. 19, no. 1, pp. 27-49: Wiley Online Library.
[41] M. Segev-Bar, A. Landman, M. Nir-Shapira, G. Shuster, H. J. A. a. m. Haick, and interfaces, "Tunable touch sensor and combined sensing platform: toward nanoparticle-based electronic skin," vol. 5, no. 12, pp. 5531-5541, 2013.
[42] S. Y. Han, K. S. Jeon, B. Cho, M. S. Seo, J. Song, and H.-S. J. I. J. o. Q. E. Kong, "Characteristics of a-SiGe: H thin film transistor infrared photosensor for touch sensing displays," vol. 48, no. 7, pp. 952-959, 2012.
[43] Y. Yang et al., "Electret film-enhanced triboelectric nanogenerator matrix for self-powered instantaneous tactile imaging," vol. 6, no. 5, pp. 3680-3688, 2014.
[44] X. Pu, S. An, Q. Tang, H. Guo, and C. J. I. Hu, "Wearable triboelectric sensors for biomedical monitoring and human-machine interface," p. 102027, 2021.
[45] M. I. Tiwana, S. J. Redmond, N. H. J. S. Lovell, and A. A. physical, "A review of tactile sensing technologies with applications in biomedical engineering," vol. 179, pp. 17-31, 2012.
[46] H.-E. Endres, S. J. S. Drost, and A. B. Chemical, "Optimization of the geometry of gas-sensitive interdigital capacitors," vol. 4, no. 1-2, pp. 95-98, 1991.
[47] N. Angkawisittpan and T. J. M. S. R. Manasri, "Determination of sugar content in sugar solutions using interdigital capacitor sensor," vol. 12, no. 1, p. 8, 2012..